Available online at www.sciencedirect.com
SCIENCE DIRECT®
Agricultural and Forest Meteorology 137 (2006) 43–55
AGRICULTURAL AND FOREST METEOROLOGY
www.elsevier.com/locate/agrformet

Improving estimation of hourly, daily, and monthly solar radiation by importing global data sets

Kun Yang [a,*], Toshio Koike [a], Baisheng Ye [b]

[a] Department of Civil Engineering, The University of Tokyo, Tokyo, Japan
[b] Cold and Arid Regions Environmental and Engineering Research Institute, Chinese Academy of Science, Lanzhou, China

Received 17 February 2005; received in revised form 8 February 2006; accepted 24 February 2006

Abstract

Surface solar radiation is an important parameter in hydrological models and crop yield models. This study developed a model to estimate solar radiation from sunshine duration. The model is more accurate and more general than traditional Ångström–Prescott models. It can explicitly account for radiative extinction processes in the atmosphere. Moreover, global data sets that describe the spatial and temporal distribution of ozone thickness and Ångström turbidity were introduced in the model to enhance its universal reliability and applicability. The model was calibrated in lowland and humid sites and validated at a number of sites in various climate and elevation regions. The new model shows overall better performances than three Ångström–Prescott models. Because this model follows the simple form of the Ångström–Prescott model, and its inputs (sunshine duration, air temperature, and relative humidity) are accessible from routine surface meteorological observations, it can be easily applied to hydrological and agricultural studies. The source code and the auxiliary data of the model are available from the authors upon request.

Keywords: Solar radiation; Transmissivity; Ozone; Turbidity; Sunshine duration

1. Introduction

Models for irrigation scheduling, crop growth, and hydrological cycles are driven by surface meteorological data. Some parameters such as precipitation and temperature are widely available. By contrast, the direct measurements of surface solar radiation are very sparse in most regions (Hunt et al., 1998; Liu and Scott, 2001), especially in highland and mountainous regions. Because solar radiation provides the energy for the processes that drive photosynthesis and evapotranspiration, it is an indispensable parameter for many hydrological and agricultural studies (Cooter and Dhakhwa, 1995; Hunt et al., 1998; Hoogenboom, 2000; Pohlert, 2004). In order to meet the needs of these studies, several approaches have been developed for estimating the surface solar radiation, such as remote sensing retrievals (Pinker et al., 1994, 1995), single-layer and multi-layer radiativer transfer models (Bird, 1984; Berk et al., 1989; Gueymard, 1995; Pawlak et al., 2004), and a number of empirical models based on surface meteorological data. In hydrological and agricultural studies, the empirical models are most popular, because of its low computational cost and accessible inputs.

The empirical models can be roughly classified into three categories, i.e. sunshine-based models (Ångström, 1924; Prescott, 1940), temperature-based models (Bristow and Campbell, 1984; Thornton and Running, 1999; Meza and Varas, 2000; Weiss and Hays, 2004), and cloud-based models (Nielsen et al., 1981; Supit and van Kappel, 1998; Ehnberg and Bollen, 2005). The

* Corresponding author at: River Lab, Department of Civil Engineering, University of Tokyo, Hongo 7-3-1, Bunkyo-Ku, Tokyo 113-8656, Japan. Tel.: +81 3 5841 6109; fax: +81 3 5841 6130.
E-mail address: yangk@hydra.t.u-tokyo.ac.jp (K. Yang).

0168-1923/$ – see front matter
doi:10.1016/j.agrformet.2006.02.001

Nomenclature

a, b	coefficients
g	the acceleration of gravity (9.81 m s^{-2})
h	solar elevation (radian)
h_r	surface air relative humidity (%)
H_T	scale height of an isothermal atmosphere (m)
I_b	solar direct normal irradiance (W m^{-2})
$I_{b,th}$	threshold value of direct normal irradiance to define sunshine duration (W m^{-2})
I_0	solar irradiance at the top of the atmosphere (W m^{-2})
l	thickness of the ozone layer (cm)
m	air mass
m_c	pressure-corrected air mass
n	sunshine duration (h)
N	the maximum possible sunshine duration (h)
p	empirical constant
p_s	surface pressure (Pa)
p_0	standard atmospheric pressure (1.013×10^5 Pa)
q	empirical constant
q_v	air specific humidity (kg kg^{-1})
R	surface solar radiation (J m^{-2})
R_{clear}	surface solar radiation under clear skies (J m^{-2})
R_0	solar radiation at the top of the atmosphere (J m^{-2})
t	time (s)
T_a	surface air temperature (K)
ΔT	period for integrating solar radiation (s)
w	precipitable water (cm)
z	altitude (m)

Greek letters

α	Ångström exponent
β	Ångström turbidity coefficient
δ	aerosol optical depth
λ	wavelength (μm)
τ	radiative transmittance in Ångström-type model
τ_a	radiative transmittances due to aerosol extinction
$\tau_{b,clear}$	solar beam radiative transmittance under clear skies
τ_c	radiative transmittance due to cloud extinction
$\tau_{d,clear}$	solar diffuse radiative transmittance under clear skies
τ_g	radiative transmittances due to permanent gas absorption
τ_{oz}	radiative transmittances due to ozone absorption
τ_r	radiative transmittances due to Rayleigh scattering
τ_w	radiative transmittances due to water vapour absorption
ϕ	latitude (°)

famous Ångström–Prescott models (hereafter A–P model) are sunshine-based and have been widely applied to estimating solar radiation for hydrological and agricultural modelling. A well-calibrated A–P model is usually more accurate than a temperature-based model and a cloud-based model (Iziomon and Mayer, 2001; Pohlert, 2004). A number of studies have focused on tuning the parameters in A–P models (e.g. Sahin and Sen, 1998; Podestá et al., 2004), and show that the parameters can be quite different in distinct regions. This is not surprising, because the A–P models do not physically account for radiative extinction processes in the atmosphere, and thus the model parameters have to be calibrated locally.

In this study, we make efforts to improve solar radiation estimation under a more general framework. The paper is organised as follows. The new model is presented in Section 2, and its inputs are described in Section 3. In Section 4, the model is calibrated using hourly, daily and monthly data in Japan. Section 5 compares this model with the FAO (Food and Agricultural Organisation) model, the Gopinathan general model (1988), and a Japan-based A–P model. The data used for the comparisons are collected in China, USA, and Saudi Arabia, which cover distinct climate and elevation regions. The availability and accuracy of input sunshine data are discussed in Section 6 and conclusions are given in Section 7.

2. Development of the new solar radiation model

The new model uses two radiative transmittances. One is a transmittance for clear sky. It is based on local geographical and meteorological conditions. The other is a cloud-related transmittance function based on hourly, daily or monthly relative sunshine duration.

2.1. Radiative transmittance for clear skies

The surface solar radiation is affected by a number of extinction processes in the atmosphere. Many spectral

models (e.g. Bird, 1984; Dozier, 1980) can be used for calculating solar spectral transmittance in clear skies. Yang et al. (2001) developed a broadband radiative transfer model by simplifying Leckner's spectral model (1978). Gueymard (2003a,b) evaluated 21 models and concluded that this broadband model was one of the best broadband models that is comparable to spectral radiative transfer models for calculating beam irradiance under clear skies. Paulescu and Schlett (2003, 2004) and Madkour et al. (2006) also verified the high performance of this model. Therefore, this study uses it to calculate solar beam radiative transmittance $\tau_{b,clear}$ and solar diffuse radiative transmittance $\tau_{d,clear}$ under clear skies. Because there was a typewriting error in Yang et al. (2001), we rewrite this model here:

$$\tau_{b,clear} \approx \max(0, \tau_{oz}\tau_w\tau_g\tau_r\tau_a - 0.013), \quad (1a)$$

$$\tau_{d,clear} \approx \max\{0, 0.5[\tau_{oz}\tau_g\tau_w(1 - \tau_a\tau_r) + 0.013]\}, \quad (1b)$$

$$\tau_g = \exp(-0.0117 m_c^{0.3139}), \quad (1c)$$

$$\tau_r = \exp[-0.008735 m_c (0.547 + 0.014 m_c - 0.00038 m_c^2 + 4.6 \times 10^{-6} m_c^3)^{-4.08}], \quad (1d)$$

$$\tau_w = \min[1.0, 0.909 - 0.036 \ln(mw)], \quad (1e)$$

$$\tau_{oz} = \exp[-0.0365 (ml)^{0.7136}], \quad (1f)$$

$$\tau_a = \exp\{-m\beta[0.6777 + 0.1464(m\beta) - 0.00626(m\beta)^2]^{-1.3}\}, \quad (1g)$$

$$m = 1/[\sin h + 0.15(57.296h + 3.885)^{-1.253}], \quad (1j)$$

$$m_c = m p_s / p_0, \quad (1k)$$

where τ_g, τ_r, τ_w, τ_{oz}, and τ_a are the broadband radiative transmittances due to permanent gas absorption, Rayleigh scattering, water vapour absorption, ozone absorption, and aerosol extinction, respectively. m is the air mass, m_c the pressure-corrected air mass, h (radian) the solar elevation, and $p_0 = 1.013 \times 10^5$ Pa. Compared with A–P models, the new model requires four additional parameters, i.e. the surface pressure p_s (Pa), the precipitable water w (cm), the thickness of the ozone layer l (cm or 1000 Dobson Units), and the Ångström turbidity coefficient β.

2.2. A radiative transmittance for cloudy condition

The transmittance due to cloud extinction is defined as the ratio of surface solar radiation R (J m^{-2}) to that under clear skies R_{clear} (J m^{-2}), i.e.

$$\tau_c \equiv R/R_{clear}. \quad (2)$$

Because the effects of other factors (such as Rayleigh scattering and aerosol extinction) on radiative extinction have been represented in Eqs. (1a)–(1k), it is reasonable to assume that the radiative extinction in cloud layers is a function of sunshine duration (Ångström, 1924). In other words, τ_c can be described as $f(n/N)$. Herein, n is the actual sunshine duration, and N is the maximum possible sunshine duration.

2.3. Global solar radiation model

Once the radiative transmittances for clear skies and for cloud layers are available, the global solar radiation R (J m^{-2}) can be calculated by

$$R = \tau_c \int_{\Delta T} (\tau_{b,clear} + \tau_{d,clear}) I_0 \, dt, \quad (3)$$

where I_0 (W m^{-2}) is the solar irradiance on a horizontal surface at the top of the atmosphere, t (s) the time, ΔT (s) the integration period, and the integral part is R_{clear}, the surface solar radiation under clear skies.

3. Description of input parameters

In order to estimate global solar radiation, the new model needs to input sunshine duration, surface pressure, precipitable water, ozone thickness, and Ångström turbidity coefficient. The following subsections introduce how to obtain their values from basic surface meteorological data and geographical data.

3.1. Relative sunshine duration

Both A–P models and the new model need the relative sunshine duration (or the fraction of sunshine duration) n/N. The sunshine duration n is usually measured by a sunshine recorder at meteorological stations, while the maximum possible sunshine duration N is usually not available. In A–P models, N is simply

replaced by the length of time for which solar irradiance is observable. For daily solar radiation estimation, N is the daylength (Martinez-Lozano et al., 1984). However, according to the definition by The World Meteorological Organization (WMO) in 1981, the sunshine duration is the length of time for which solar direct normal irradiance (I_b) exceeds a threshold value of 120 W m^{-2}. The replacement of N by the daylength in an A–P model would overestimate the maximum possible sunshine duration, because the ground-received I_b near sunrise and sunset cannot exceed 120 W m^{-2}. In the new model, the broadband model in Section 2 can be used to calculate the I_b under clear skies (i.e. $I_b = \tau_{b,clear} I_0 / \sin h$, h is the solar elevation) and thus output the true value of the maximum possible sunshine duration. This is one of merits of the new model.

3.2. Surface pressure

The surface pressure is usually measured at meteorological stations. If it is not available, we can estimate it by

$$p_s = p_0 \exp(-z/H_T), \tag{4}$$

where $p_0 = 1.013 \times 10^5$ Pa, z (m) is the altitude, and H_T (m) is the scale height of an isothermal atmosphere.

Given the scale height $H_T = 8430$ m, Eq. (4) can give a good estimate of mean surface pressure. The surface pressure, or the corrected air mass m_c in Eq. (1k), decreases quickly with respect to the elevation, which in turn affects the radiative extinctions due to Rayleigh scattering and permanent gas absorption. While the gas absorption contributes little to radiative extinction, the Rayleigh scattering can significantly change the radiative transmittance. Therefore, increasing surface elevation would lead to a high radiative transmittance.

3.3. Precipitable water

The precipitable water is defined as the amount of water in a vertical column of atmosphere, i.e.

$$w \equiv (1/g) \int_0^{p_s} q_v \, \mathrm{d}p, \tag{5}$$

where $g = 9.81$ m s^{-2}, and q_v (kg kg^{-1}) is the specific humidity.

Calculating the precipitable water needs humidity profile measurements of the atmosphere, which is usually unavailable at surface meteorological stations. In this model, the precipitable water w (cm) is estimated from surface relative humidity h_r (%) and air temperature T_a (K) by a semi-empirical formula:

$$w = 0.00493 h_r T_a^{-1} \exp[26.23 - 5416 T_a^{-1}]. \tag{6}$$

The precipitable water can approach zero in a dry environment (e.g. over desert areas) while exceed 5 cm in a humid environment (e.g. over tropical oceans). According to Eq. (1e), the transmittance may approach unity in a dry atmospheric environment while decreasing to 0.8 in a moist atmospheric environment, indicating that water vapour absorption plays a significant role in radiative extinction.

3.4. Global distribution of ozone thickness

The ozone thickness generally increases toward high latitudes except near the South Pole. Also, it has seasonal variations, being higher in the spring and lower in the autumn. In Yang et al. (2001) and Yang and Koike (2002), the ozone thickness is roughly estimated by an empirical formula. In the new model, the values of ozone thickness are based on the satellite products provided by NASA/GSFC Ozone Processing Team. The team accumulated data sets of the ozone thickness for 24 years, i.e. Nimbus 7 TOMS (Total Ozone Mapping Spectrometer) zonal means from 1978 to 1993 and Earth Probe TOMS zonal means from 1996 to 2003. Here, the zonal mean is an average of the total column ozone through a single global latitude band. The temporal resolution of the data sets is monthly, and spatial resolution is 5° from south to north (see http://toms.gsfc.nasa.gov/ozone/ozone_v8.html). Using these data sets, we created a decadal mean data set for ozone thickness, which has the same temporal (monthly) and spatial (5°) resolution as the original satellite products. Fig. 1 shows the distribution of the composite ozone thickness. It clearly shows the ozone hole in the South Pole and a general tendency of the zone thickness increasing with latitude.

3.5. Global distribution of Ångström turbidity coefficient

In general, the turbidity coefficient decreases with respect to elevation and latitude, and Ångström (1961) proposed an empirical formula to estimate its zonal mean value, which was used in Yang et al. (2001) and Yang and Koike (2002). However, it can be questionable in some areas because of the high variability of the turbidity in both space and time. Since there is no observed global data set for the turbidity coefficient, we alternatively derive it from aerosol optical depth (AOD), which has been investigated widely.

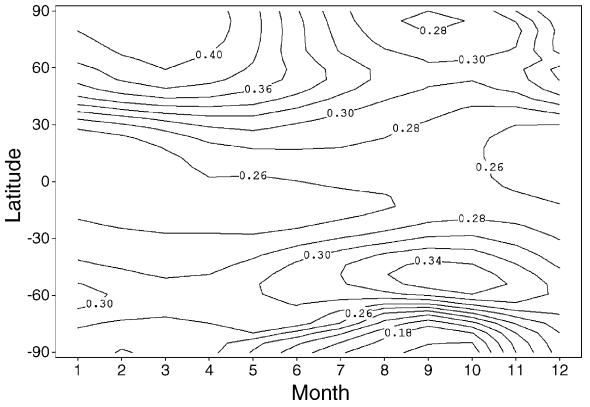

Fig. 1. Zonally averaged, column integrated seasonal cycle of the ozone thickness. Data are averaged over 10-year observations of NASA/TOMS (Total Ozone Mapping Spectrometer). The unit is cm (1000 Dobson Units). The months run from 1 = January to 12 = December.

The aerosol optical depth is wavelength-dependent, and this dependence can be expressed by

$$\delta(\lambda) = \beta\lambda^{-\alpha}, \tag{7}$$

where λ (μm) is the wavelength, $\delta(\lambda)$ the AOD value, β the Ångström turbidity coefficient, and α is the Ångström exponent.

In our radiation model (also see Leckner, 1978), the Ångström turbidity coefficient is defined at a wavelength $\lambda = 0.5$ μm with Ångström exponent $\alpha = 1.3$. That is,

$$\beta = 0.5^{1.3}\delta(0.5), \tag{8}$$

where $\delta(0.5)$ is the AOD value at $\lambda = 0.5$ μm.

There are several satellite data sources for AOD values. The AVHRR (the Advanced Very High Resolution Radiometer) AOD products only cover the oceans. The TOMS products reported values at wavelength $\lambda = 0.38$ μm rather than $\lambda = 0.5$ μm. Therefore, they are not usable for deriving the required turbidity coefficient in this model. Here, we use a software package – GADS (Global Aerosol Data Set 2.2a) – to calculate the global distribution of the aerosol optical depth. The GADS was developed at Max-Planck-Institut (Koepke et al., 1997; Hess et al., 1998), and it is a completely revised version of the aerosol climatology by d'Almeida et al. (1991). The GADS can calculate global distribution of radiative properties (such as the extinction, scattering, absorption coefficients, optical depth, and so on) at $5^\circ \times 5^\circ$ latitude–longitude grids for winter (September–February) and summer (March–August). To calculate the aerosol optical depth, we need to input three parameters: the wavelength (61 wavelengths between 0.3 and 40 μm), the season (winter or summer), and the relative humidity (eight values over 0–99%). Using this program, we at first produced 16 global data sets for the aerosol optical depth at $\lambda = 0.5$ μm, corresponding to 16 combinations of two values of season (winter or summer) and eight values of relative humidity (0%, 50%, 70%, 80%, 90%, 95%, 98%, or 99%). As an example, Fig. 2 shows the global distribution of the calculated turbidity coefficient corresponding to one combination (winter season, 90% relative humidity). The low turbidity in the Tibetan Plateau and high turbidity in the Sahara Desert and East China can be

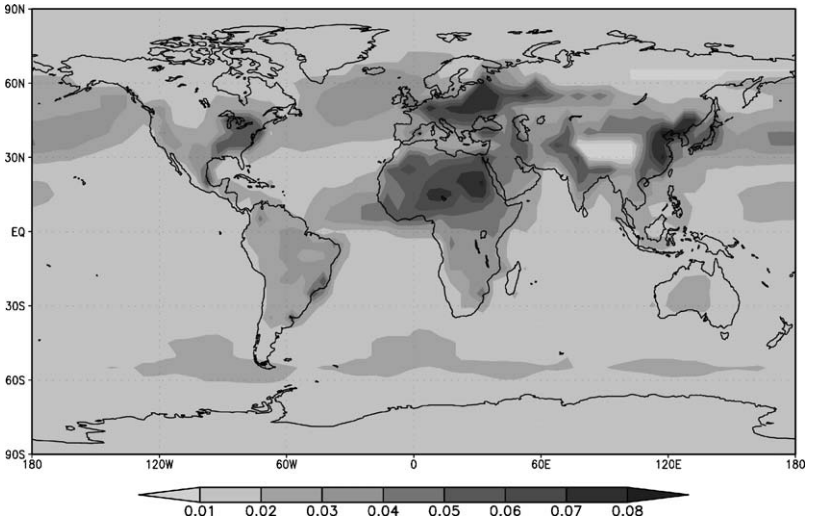

Fig. 2. The world-wide distribution of the Ångström turbidity coefficient in winter season (September–February) for a relative humidity of 90%. The values are calculated using the Global Aerosol Data Set 2.2a, Max-Planck-Institut für Meteorologie.

Table 1
Statistical geographical and annual-mean climatological data at calibration stations in Japan

Range	Altitude (m)	Latitude (°N)	Longitude (°E)	T_a (K)	h_r (%)	R (MJ m^{-2})
Minimum	0	24	124	279	55	10.80
Maximum	610	45	154	299	75	16.58

T_a, air temperature; h_r, relative humidity; R, daily global solar radiation.

recognized. In the radiation model, the AOD value at a specific season and relative humidity is interpolated from the global data sets, and converted to the turbidity coefficient β according to Eq. (8).

4. New model calibration

The transmittance τ_c due to cloud extinction is calibrated from the data in Japan. The Japan Meteorological Agency maintains 67 stations with the measurements of hourly air temperature, relative humidity, sunshine duration, and solar radiation. Table 1 shows that these stations have similar geographical (low elevation) and climatological (humid) characteristics.

We use a two-pass procedure to calibrate the model: select data in pass one and calibrate model in pass two. In pass one, an A–P model for daily solar radiation estimation is preliminarily calibrated using all the data in 1995. The root mean square error (RMSE) was evaluated at individual stations. In pass two, we excluded the stations with RMSE > 2.0 MJ m^{-2}, and the remaining stations were used for the model calibration here. The calibrated cloud-related transmittance for hourly solar radiation estimation is

$$\tau_c = \begin{cases} 0.4435 + 0.3976\dfrac{n}{N} + 0.1589\left(\dfrac{n}{N}\right)^2 & \text{if } n > 0 \\ 0.2560 \quad \text{if } n = 0 \end{cases} \tag{9a}$$

For daily solar radiation estimation,

$$\tau_c = 0.2505 + 1.1468n/N - 0.3974(n/N)^2. \tag{9b}$$

And for monthly mean daily solar radiation estimation:

$$\tau_c = 0.2777 + 0.8636n/N - 0.1413(n/N)^2. \tag{9c}$$

The above calibration is constrained by a condition that $\tau_c = 1$ if $n/N = 1$, which is implied in the definition of the cloud-related transmittance (see Eq. (2)).

Note that n/N in Eqs. (9a)–(9c) represents the relative sunshine duration during a certain period ΔT (hourly, daily, or monthly). Also, the cloud-related transmittance is expressed by a nonlinear formula of the relative sunshine duration rather than a linear formula, as suggested by Iqbal (1979) and Suehrcke (2000).

5. Model comparisons

5.1. Models

To compare with the new model, three models were selected: the FAO A–P model, and the Gopinathan A–P model (1988), and a locally calibrated A–P model. The A–P models have the following form:

$$R = \tau \int_{\Delta T} I_0 \, dt, \tag{10}$$

where τ is the total transmittance accounting for all the radiative extinctions in the atmosphere.

In the FAO model:

$$\tau = (0.25 + 0.5n/N). \tag{11}$$

Gopinathan (1988) proposed the following formulas based on widely distributed data:

$$\tau = (a + bn/N). \tag{12a}$$

$$a = -0.309 + 0.539\cos\phi - 6.93 \times 10^{-5} z + 0.290n/N, \tag{12b}$$

$$b = 1.529 - 1.027\cos\phi + 9.26 \times 10^{-5} z - 0.359n/N, \tag{12c}$$

where z (m) is the altitude, and ϕ (°) is the latitude.

In addition, we regressed an A–P model from the data in Japan. For hourly solar radiation estimation:

$$\tau = \begin{cases} 0.3038 + 0.4133\dfrac{n}{N} + 0.0138\left(\dfrac{n}{N}\right)^2 & \text{if } n > 0 \\ 0.1811 \quad \text{if } n = 0 \end{cases} \tag{13a}$$

For daily solar radiation estimation:

$$\tau = 0.1707 + 0.9253n/N - 0.4027(n/N)^2. \tag{13b}$$

And for monthly mean daily solar radiation estimation:

$$\tau = 0.2043 + 0.6176n/N - 0.0954(n/N)^2. \tag{13c}$$

The three models were used to estimate daily and monthly mean daily solar radiation, and the Japan-based

A–P model was also used to estimate hourly solar radiation. Model performances were evaluated by the mean bias error (MBE) and root mean square error (RMSE).

5.2. Data

The four models were tested at seven stations in China, seven in USA, and 12 in Saudi Arabia. Table 2 lists the geographical and annual-mean climatological data at these stations. Compared with the humid and lowland calibration stations in Japan, the validation stations have diverse climate regimes (from humid to dry) and widely varying elevations (from the sea level up to thousands of metres). The data in China were collected at surface meteorological stations maintained by Chinese Meteorological Administration. At these stations, daily surface pressure, air temperature, specific humidity, sunshine duration, and global solar radiation were measured. The data in 1997–1998 were used for the comparisons. The data in USA and in Saudi Arabia were obtained by the Cooperative Network for Renewable Resource Measurements (CONFRRM) and a NASA Remote Sensing Validation project, respectively. At these stations, the global horizontal irradiance, direct normal irradiance, air temperature, and relative humidity were measured in an interval of 5 min. Because sunshine data were not measured, we estimated their values from the measured direct normal irradiance according to its definition by the WMO (see Section 3.1). The data in 1998 were used for the model comparisons.

5.3. Results

The MBE and RMSE in estimating hourly, daily, and monthly mean daily global radiation are shown in Tables 3–5, respectively. These tables show that all the radiation models tend to produce larger errors in humid regions than in dry regions and thus the model accuracy may be related to climate regimes. In addition, all the models produced large errors for China stations while small errors for USA and Saudi Arabia stations. Possibly, the routinely observed data in China have larger errors than the instrumental data in USA and Saudi Arabia.

Table 2
Geographical and annual-mean climatological data at validation stations in China, USA, and Saudi Arabia

Region (period)	Station	Altitude (m)	Latitude (°N)	Longitude (°E)	T_a (K)	h_r (%)	R (MJ m^{-2})
China (1997, 1998)	Sanya	6	18.23	109.52	300.4	76	16.63
	Beijing	55	39.93	116.28	287.2	55	13.69
	Chengdu	507	30.67	104.02	290.5	77	8.50
	Kashi	1291	39.47	75.98	284.9	54	15.05
	Kunming	1897	25.02	102.68	289.3	67	15.26
	Germu	2809	36.42	94.9	279.1	33	18.81
	Lhasa	3659	29.72	91.03	280.8	49	20.60
USA (1998)	Elizabeth city (EC)	26	36.28	−76.22	291.2	74	14.98
	Edinburgh (ED)	30	26.2	−98.22	299.3	66	16.55
	Clear lake/NASA (CL)	33	29.56	−95.12	296.5	75	15.63
	Austin (AU)	213	30.29	−97.74	296.6	63	15.86
	Canyon (CN)	1067	34.99	−101.9	290.8	51	15.43
	Southwest Technology Development Institute (ST)	1201	32.27	−106.74	295.6	33	18.49
	El Paso (EP)	1219	31.8	−106.4	294.3	32	20.68
Saudi Arabia (1998)	Jeddah (JN)	4	21.68	39.15	303.8	55	21.47
	Gizan (GN)	7	16.9	42.58	304.7	72	10.53
	Al-Ahsa (AH)	178	25.3	49.48	303.9	23	21.60
	Al-Qaisumah (QA)	358	28.32	46.13	301.7	30	21.21
	Al-Madinah (MA)	626	24.55	39.7	304.3	23	21.98
	Qassim (GS)	647	26.31	43.77	301.3	27	21.55
	Solar village (SV)	650	24.91	46.41	301.1	30	21.30
	Al-Jouf (SK)	669	29.79	40.1	298.4	33	21.80
	Wadi Al-Dawaser (WD)	701	20.44	44.68	303.9	25	22.71
	Sharurah (SH)	725	17.47	47.11	304.4	24	23.44
	Tabouk (TB)	768	28.38	36.61	298.2	31	21.55
	Abha (AB)	2039	18.23	42.66	294.2	51	22.10

Stations in each region are listed in increasing order of altitude (third column). T_a, air temperature; h_r, relative humidity; R, daily global solar radiation.

Table 3
Performances of the Japan-based Ångström–Prescott model (“A–P”) and the new model (“New”) in estimating hourly mean solar irradiance at validation stations in USA and Saudi Arabia

Region (period)	Station	Altitude (m)	MBE (W m^{-2})		RMSE (W m^{-2})	
			A–P	New	A–P	New
USA (1998)	EC	26	10	5	66	**65**
	ED	30	47	48	**79**	80
	CL	33	34	25	73	**68**
	AU	213	32	33	69	**68**
	CN	1067	5	23	60	**56**
	ST	1201	−24	5	76	**51**
	EP	1219	−11	18	63	**54**
Saudi Arabia (1998)	JN	4	18	6	55	**46**
	GN	7	27	15	61	**53**
	AH	178	2	24	**54**	60
	QA	358	−6	2	55	**47**
	MA	626	−1	9	53	**40**
	GS	647	0	13	53	**41**
	SV	650	−5	−4	57	**42**
	SK	669	0	14	56	**46**
	WD	701	1	14	49	**39**
	SH	725	−13	7	59	**53**
	TB	768	−1	1	52	**38**
	AB	2039	−16	−4	67	**47**

MBE, mean bias error; RMSE, root mean square error. Bold values are the minimum RMSE.

Table 3 shows the errors of hourly irradiance estimation for USA and Saudi Arabia stations (hourly solar radiation at the China stations are not available). Evidently, the new model and the A–P model usually yield similar MBE values for the estimation of hourly radiation, but the former gives smaller RMSE values (bold values) and higher correlation coefficients (not shown) at almost all the stations, indicating that the new model is more reasonable for hourly solar radiation estimation than the A–P model. This is not unexpected. Hourly radiation is not only determined by the daytime variation of the extraterrestrial solar radiation but also by the daytime variation of radiative transmittance (i.e. low transmittance in the early morning and late afternoon while high transmittance near noon). The A–P model does not account for the daytime variation of the radiative transmittance, while the new model has explicitly accounted for it. As an example, Fig. 3 shows a scatterplot between the measured and estimated hourly radiation for a lowland site (Saudi Arabia/JN, 4 m). The A–P model overestimates the radiation in the early morning and in the late afternoon (see points with low radiation values in Fig. 3) and underestimates the radiation near noon (see points with high radiation values in Fig. 3), while the new model works well throughout the daytime. Accordingly, the A–P model always yields higher RMSE values than the new model, even though it can yield small MBE values, as shown in Table 3.

Table 4 shows that the new model yields the smallest RMSE values at most of USA and Saudi Arabia stations and at half of China stations for the estimation of daily radiation. In particularly, at high stations ST (1201 m), AB (2039 m), Germu (2809 m), and Lhasa (3659 m), the new model performs much better than the A–P models. The latter ones significantly underestimate radiation at these stations, as indicated by the large negative bias values in Table 4. As an example, Fig. 4 shows a scatterplot for daily radiation at a highland site (Saudi Arabia/AB, 2039 m). The difference performance can be explained as follows. The air mass, precipitable water, and turbidity at highland sites are relatively small compared to lowland sites, and therefore the radiative transmittance is relatively high. This fact has been automatically taken into account in the new model, but the A–P models are not able to deal with it.

Table 5 also shows that the new model performs better than the A–P models in estimating monthly mean daily radiation. The new model yields the minimum or the second minimum RMSE values at most of the stations.

Table 4
Performances of the FAO model (“FAO”), Gopinathan model (“GM”), Japan-based Ångström–Prescott model (“A–P”), and the new model (“New”) in estimating daily solar radiation at validation stations in China, USA, and Saudi Arabia

Region (period)	Station	Altitude (m)	MBE (MJ m^{-2})				RMSE (MJ m^{-2})			
			FAO	GM	A–P	New	FAO	GM	A–P	New
China (1997, 1998)	Sanya	6	−0.65	−0.51	−0.75	−0.79	2.81	**2.79**	3.03	2.99
	Beijing	55	1.34	1.46	1.17	0.78	2.34	2.93	2.40	**2.16**
	Chengdu	507	2.73	0.63	1.66	1.80	3.59	**3.05**	3.08	3.12
	Kashi	1291	1.41	1.73	1.35	1.89	**2.10**	3.54	2.30	2.67
	Kunming	1897	0.59	−1.16	0.23	0.76	2.41	3.12	**2.25**	2.33
	Germu	2809	−1.05	−0.72	−1.13	0.65	2.07	2.78	2.26	**1.75**
	Lhasa	3659	−2.66	−3.32	−2.42	−0.97	3.27	4.82	3.14	**2.16**
USA (1998)	EC	26	0.30	0.30	0.14	−0.14	2.33	1.97	1.92	**1.80**
	ED	30	2.16	2.14	1.92	1.94	2.59	2.61	2.46	**2.40**
	CL	33	1.71	1.66	1.41	1.10	2.36	2.35	2.25	**1.90**
	AU	213	1.60	1.47	1.24	1.28	2.20	2.09	2.01	**1.87**
	CN	1067	0.73	0.97	0.15	0.95	1.74	1.91	1.71	**1.65**
	ST	1201	−0.78	−0.27	−1.39	−0.06	1.76	1.51	2.31	**1.33**
	EP	1219	−0.06	0.42	−0.70	0.64	**1.17**	1.30	1.69	1.34
Saudi Arabia (1998)	JN	4	0.62	0.28	0.27	−0.12	1.52	1.28	1.28	**1.17**
	GN	7	0.77	0.50	0.74	0.21	1.19	1.23	1.25	**0.92**
	AH	178	0.06	−0.11	−0.42	0.62	1.32	**1.14**	1.25	1.45
	QA	358	−0.39	−0.29	−0.82	−0.33	1.62	1.36	1.58	**1.28**
	MA	626	−0.04	−0.15	−0.54	0.10	1.28	1.16	1.36	**1.02**
	GS	647	0.18	0.08	−0.48	0.34	1.11	**1.01**	1.22	1.03
	SV	650	0.13	0.29	−0.64	−0.25	1.03	1.05	1.43	**1.01**
	SK	669	0.22	0.02	−0.44	0.40	1.06	**1.00**	1.27	1.01
	WD	701	0.22	−0.28	−0.46	0.41	0.96	**0.93**	1.10	**0.93**
	SH	725	−0.93	−1.28	−1.18	−0.28	1.85	1.84	1.76	**1.28**
	TB	768	0.14	0.36	−0.46	−0.11	1.27	1.24	1.44	**1.10**
	AB	2039	−0.77	−0.99	−0.85	−0.28	1.42	1.59	1.81	**1.35**

MBE, mean bias error; RMSE, root mean square error. Bold values are the minimum RMSE.

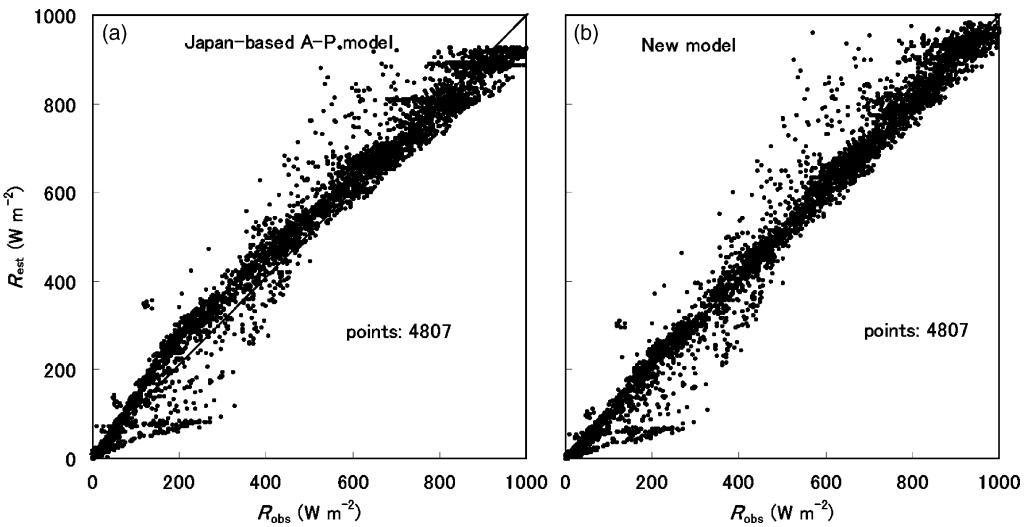

Fig. 3. Comparison between observed (R_{obs}) and estimated (R_{est}) hourly mean solar irradiance at a lowland site (Saudi Arabia/JN, z = 4 m) for 1998.

Table 5
Same as Table 4 but for monthly mean daily solar radiation

Region (period)	Station	Altitude (m)	MBE (MJ m^{-2})				RMSE (MJ m^{-2})			
			FAO	GM	A–P	New	FAO	GM	A–P	New
China (1997, 1998)	Sanya	6	−0.64	0.28	−1.12	−1.21	1.51	**1.36**	1.85	1.86
	Beijing	55	1.36	2.36	1.06	0.60	1.61	2.62	1.33	**1.10**
	Chengdu	507	2.80	1.42	2.02	1.99	2.86	**1.65**	2.09	2.07
	Kashi	1291	1.41	2.34	1.11	1.48	**1.63**	2.57	1.39	1.71
	Kunming	1897	0.68	−0.24	0.20	0.58	1.12	1.39	**0.76**	0.91
	Germu	2809	−1.05	−0.17	−1.37	0.02	1.30	0.72	1.60	**0.52**
	Lhasa	3659	−2.66	−2.88	−3.00	−1.87	2.85	3.64	3.20	**2.18**
USA (1998)	EC	26	0.30	1.24	−0.01	−0.31	**1.00**	1.57	1.01	1.03
	ED	30	2.15	2.95	1.80	1.62	2.23	3.01	1.88	**1.70**
	CL	33	1.71	2.68	1.38	0.98	1.76	2.76	1.44	**1.07**
	AU	213	1.58	2.48	1.25	1.10	1.63	2.54	1.32	**1.16**
	CN	1067	0.66	1.70	0.29	0.73	**0.98**	1.86	0.87	1.00
	ST	1201	−0.80	0.15	−1.25	−0.44	1.12	0.69	1.54	**0.65**
	EP	1219	−0.07	0.80	−0.51	0.28	**0.32**	0.85	0.68	0.42
Saudi Arabia (1998)	JN	4	0.62	0.48	0.16	−0.50	0.85	0.71	**0.62**	0.70
	GN	7	0.77	0.70	0.34	−0.35	0.87	0.90	**0.51**	0.52
	AH	178	0.06	0.16	−0.41	0.06	0.59	**0.51**	0.74	0.69
	QA	358	−0.39	0.06	−0.82	−0.65	0.94	**0.81**	1.22	0.94
	MA	626	−0.03	0.10	−0.50	−0.25	0.75	**0.63**	0.94	0.65
	GS	647	0.18	0.37	−0.31	0.08	0.57	0.64	0.68	**0.53**
	SV	650	0.13	0.57	−0.36	−0.40	**0.59**	0.83	0.79	0.65
	SK	669	0.22	0.33	−0.27	0.13	0.55	0.60	0.63	**0.33**
	WD	701	0.22	−0.10	−0.31	0.06	0.49	0.44	0.56	**0.33**
	SH	725	−0.92	−1.09	−1.38	−0.87	1.04	1.19	1.47	**0.94**
	TB	768	0.14	0.52	−0.35	−0.35	0.83	0.89	0.94	**0.76**
	AB	2039	−0.77	−0.62	−1.18	−0.86	0.87	**0.77**	1.25	0.95

5.4. Statistical analysis

Because comparisons at individual stations may be contaminated by data quality of input parameters and radiation measurements, it would be reasonable to compare statistical errors among the models. Table 6 shows the statistical RMSE values according to the stations' region, altitude, and annual mean relative humidity, respectively. This table shows the following findings: (1) the new model produces the minimum

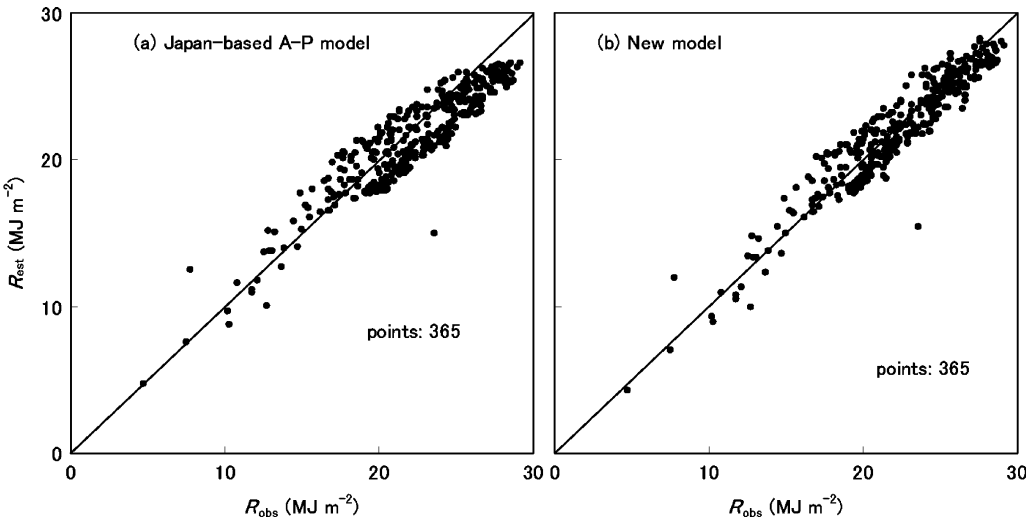

Fig. 4. Comparison between observed (R_{obs}) and estimated (R_{est}) daily solar radiation at a highland site (Saudi Arabia/AB, z = 2039 m) for 1998.

Table 6
Statistically averaged root mean square errors in estimating hourly, daily, and monthly mean daily solar radiation

	Hourly (W m^{-2})		Daily (MJ m^{-2})				Monthly mean daily (MJ m^{-2})			
	A–P	New	FAO	GM	A–P	New	FAO	GM	A–P	New
Regions										
China	–	–	2.66	3.29	2.64	**2.45**	1.84	1.99	1.75	**1.48**
USA	69	**63**	2.02	2.96	2.05	**1.76**	1.29	1.90	1.25	**1.00**
Saudi Arabia	56	**46**	1.30	1.24	1.40	**1.13**	0.75	0.74	0.86	**0.67**
All regions	61	**52**	1.86	1.98	1.91	**1.64**	1.19	1.39	1.20	**0.98**
Altitude										
<500	64	**61**	2.03	1.98	1.94	**1.79**	1.30	1.68	1.19	**1.07**
500–1000	54	**43**	1.52	1.41	1.58	**1.31**	0.96	0.86	1.01	**0.78**
1000–2000	66	**54**	**1.84**	2.28	2.05	1.86	1.03	1.47	1.05	**0.94**
>2000	67	**47**	2.25	3.06	2.40	**1.75**	1.67	1.71	2.02	**1.22**
Relative humidity										
>50%	66	**60**	2.20	2.34	2.13	**2.02**	1.50	1.91	1.26	**1.24**
<50%	57	**46**	1.52	1.63	1.68	**1.28**	0.92	0.94	1.16	**0.75**

The statistics is according to the location, altitude, and annual-mean relative humidity. "FAO", "GM", "A–P", and "New" represent four models.

regional RMSE values at all the three regions for estimating hourly, daily, and monthly radiation. Compared with the best performing A–P model, the new model can reduce the RMSE values by about 10%. (2) Model performances are elevation-dependent, and the new model is the best performer for almost all the elevation zones. The Japan-based A–P model performs well in lowland areas (<500 m), the Gopinathan model performs well for 500–1000 m high stations, and the FAO model shows good performances in 500–2000 m high stations. However, no A–P model performs well for very high stations (>2000 m), where the RMSE values given by the A–P models are 20% larger than the ones given by the new model. The A–P models tend to underestimate the radiation in highland regions, while the new model works well. (3) Model performances also depend on climate regimes, and the new model is still the best one for both dry stations (defined as annual-mean relative humidity <50%) and humid stations (defined as annual-mean relative humidity >50%). Note that the RMSE values yielded by the Japan-based A–P model are close to the ones by the new model in humid areas while much larger (20%) than the latter in dry areas. This is because the Japan-based A–P model was calibrated in humid areas. By contrast, the FAO model performs well in dry areas but not so well in humid areas.

6. Discussions

6.1. Availability of hourly sunshine data

Many sophisticated models for agricultural and hydrological studies require hourly radiation data. The estimation of hourly solar radiation needs relative sunshine duration measured over each hour, but there are more stations which report daily values of sunshine duration than hourly values. Though theoretically the hourly data could be obtained from the cards that record sunshine duration, "the transcription of hourly data can be a daunting prospect when large numbers of recording sites are involved" (Revfeim, 1997). Nevertheless, simple methods have been developed in early studies for downscaling of sunshine duration from daily values to hourly values (Revfeim, 1997).

6.2. Accuracy of sunshine data

From 1981, the WMO defined the sunshine duration as the length of time for which solar direct normal irradiance exceeds a threshold value of 120 W m^{-2}. This definition is followed in our radiation model. However, prior to 1981, a threshold value of 210 W m^{-2} was used to define the sunshine duration. Therefore, historical recorded sunshine data prior to 1981 underestimate sunshine duration using the current threshold. The measured sunshine data can be corrected by the following empirical formula (Gueymard, 1993):

$$(n/N)_{I_{b,th}} = [p + q(n/N)_{120}](n/N)_{120}, \quad (14a)$$

$$p = 1.74957 - 8.2666 \times 10^{-3} I_{b,th} + 1.6835 \times 10^{-5} I_{b,th}^2, \quad (14b)$$

$$q = -0.75072 + 8.3544 \times 10^{-3} I_{b,th} + 1.7487 \times 10^{-5} I_{b,th}^2, \quad (14c)$$

where $I_{b,th}$ (W m^{-2}) is the threshold value of direct normal irradiance for the measurement of sunshine duration, $(n/N)_{I_{b,th}}$ the measured value of n/N, and $(n/N)_{120}$ is the corrected value for threshold value of 120 W m^{-2}. Formulas for p and q are empirical constants: $p = 0.756$ and $q = 0.2325$ for $I_{b,th} = 210$ W m^{-2} (the threshold value before 1981); $p = 1$ and $q = 0$ for $I_{b,th} = 210$ W m^{-2} (the threshold value from 1981).

6.3. Comparability with remotely sensed radiation

Satellite data have been successfully used to derive the solar radiation at the Earth's surface. The RMSE values of the hourly mean irradiance estimated from the Geostationary Meteorological Satellites (GMS) range over 45–80 W m^{-2} (Kawamura et al., 1998; Perez et al., 2002). On the other hand, the present model produces RMSE values of hourly radiation in the range of 40–70 W m^{-2} in USA and Saudi Arabia (see Table 3) and about 60 W m^{-2} in Japan (not shown), which are comparable to the errors of the GMS radiation products. Therefore, the historical sunshine data, which have much longer records than the satellite data, can be used to produce long-term series of solar radiation with comparable or better accuracy.

7. Conclusions

In this study, we developed a new solar radiation model. An essential difference between the new model and the traditional A–P models lies in the parameterisation of radiative transmittance. In the A–P models, the radiative transmittance, which is merely a function of relative sunshine duration, implicitly includes all the effects of radiative extinction processes in the atmosphere, so the function is site-dependent and has to be calibrated for different climate zones and elevations. In the new model, the radiatve extinctions under clear skies and in cloudy conditions are parameterised separately. The transmittance in clear skies is explicitly and accurately parameterised based on a spectral model, and the transmittance due to cloud absorption and scattering is parameterised by the sunshine duration. Another noticeable feature is that global data sets are imported into the new model to describe the spatial and seasonal variations of the ozone thickness and turbidity coefficients. Therefore, the new model can effectively account for effects of local factors, such as elevation, turbidity, and meteorological conditions, and thus it is more physically based.

By comparisons using observations at widely distributed sites, we show that the new model improves the estimates of hourly, daily, and monthly solar radiation. It exhibits significant superiorities in modelling hourly solar radiation and general applicability in diverse climate and elevation regions. Because this model only needs to input sunshine duration, air temperature, humidity, and accessible global data sets for ozone and turbidity, it can be easily implemented for hydrological and agricultural studies. The source code and the auxiliary data of the model are available from the authors upon request.

Acknowledgements

The data used in this study were provided by Japan Meteorological Agency (JMA), Chinese Meteorological Administration (CMA), and USA Renewable Resource Data Center (RReDC). The RReDC is supported by the National Center for Photovoltaics (NCPV) and managed by the Department of Energy's Office of Energy Efficiency and Renewable Energy. The RReDC is maintained by the Electric and Hydrogen Systems Center at the National Renewable Energy Laboratory. The authors are grateful to NASA/GSFC Ozone Processing Team who provided global ozone data. They also thank Dr. Wenfeng Huang and Dr. Yanjun Shen for their helpful discussions.

References

Ångström, A., 1924. Solar and terrestrial radiation. Quart. J. Roy. Meteorol. Soc. 50, 121–125.

Ångström, A., 1961. Techniques of determining the turbidity of the atmosphere. Tellus 13, 214–223.

Berk, A., Bernstein, L.S., Robertson, D.C., 1989. MODTRAN: a moderate resolution model for LOWTRAN7, Air Force Geophy. Lab. Rep. GL-TR-89-0122, 38 pp [available from Geophysics Laboratory, Hanscom Air Force. Base, Massachusetts].

Bird, R.E., 1984. A simple solar spectral model for direct-normal and diffuse horizontal irradiance. Solar Energy 32, 461–471.

Bristow, K.L., Campbell, G.S., 1984. On the relationship between incoming solar radiation and daily maximum and minimum temperature. Agric. Forest. Meteorol. 31, 159–166.

Cooter, E.J., Dhakhwa, G.B., 1995. A solar radiation model for use in biological applications in the South and Southeastern USA. Agric. Forest. Meteorol. 79, 31–51.

d'Almeida, G.A., Koepke, P., Shettle, E.P., 1991. Atmospheric Aerosols: Global Climatology and Radiative Characteristics. A Deepak Publishing, 561 pp.

Dozier, J., 1980. A clear-sky spectral solar-radiation model for snow-covered mountainous terrain. Water Resour. Res. 16, 709–718.

Ehnberg, J.S.G., Bollen, M.H.J., 2005. Simulation of global solar radiation based on cloud observations. Solar Energy 78, 157–162.

Gopinathan, K.K., 1988. A general formula for computing the coefficients of the correlation connecting global solar radiation to sunshine duration. Solar Energy 41, 499–502.

Gueymard, C., 1993. Analysis of monthly average solar radiation and bright sunshine for different thresholds at Cape Canaveral, Florida. Solar Energy 51, 139–145.

Gueymard, C. A., 1995. SMARTS, A Simple Model of the Atmospheric Radiative Transfer of Sunshine: Algorithms and Performance Assessment. Technical Report No. FSEC-PF-270-95, Florida Solar Energy Center, Cocoa, FL, 78 p.

Gueymard, C.A., 2003a. Direct solar transmittance and irradiance predictions with broadband models. Part I. Detailed theoretical performance assessment. Solar Energy 74, 355–379.

Gueymard, C.A., 2003b. Direct solar transmittance and irradiance predictions with broadband models. Part II. Validation with high-quality measurements. Solar Energy 74, 381–395.

Hess, M., Koepke, P., Schult, I., 1998. Optical properties of aerosol and clouds: the software package OPAC. Bull. Am. Met. Soc. 79, 831–844.

Hoogenboom, G., 2000. Contribution of agrometeorology to the simulation of crop production and its applications. Agric. Forest. Meteorol. 103, 137–157.

Hunt, L.A., Kuchar, L., Swanton, C.J., 1998. Estimation of solar radiation for use in crop modeling. Agric. Forest. Meteorol. 91, 293–300.

Iqbal, M., 1979. Correlation of average diffuse and beam radiation with hours of bright sunshine. Solar Energy 23, 169–174.

Iziomon, M.G., Mayer, H., 2001. Performance of solar radiation models—a case study. Agric. Forest. Meteorol. 110, 1–11.

Kawamura, H., Tanahashi, S., Takahashi, T., 1998. Estimation of insolation over the Pacific Ocean off the Sanriku Coast. J. Oceanogr. 54, 457–464.

Koepke, P., Hess, M., Schult, I., Shettle, E.P., 1997. Global Aerosol Data Set. Max-Planck Institut für Meteorologie, Report No. 243, 44 p.

Leckner, B., 1978. The spectral distribution of solar radiation at the earth's surface-elements of a model. Solar Energy 20, 143–150.

Liu, D.L., Scott, B.J., 2001. Estimation of solar radiation in Australia from rainfall and temperature observations. Agric. Forest. Meteorol. 106, 41–59.

Madkour, M.A., El-Metwally, M., Hamed, A.B., 2006. Comparative study on different models for estimation of direct normal irradiance (DNI) over Egypt atmosphere. Renew. Energy 31, 361–382.

Martinez-Lozano, J.A., Tena, F., Onrubia, J.E., De La Rubia, J., 1984. The historical evolution of the Ångström formula and its modifications: review and bibliography. Agric. Forest. Meteorol. 33, 109–128.

Meza, F., Varas, E., 2000. Estimation of mean monthly solar global radiation as a function of temperature. Agric. Forest. Meteorol. 100, 231–241.

Nielsen, L., Prahm, L., Berkowicz, R., Conradsen, K., 1981. Net incoming radiation estimated from hourly global radiation and/or cloud observations. J. Climatol. 1, 255–272.

Paulescu, M., Schlett, Z., 2003. A simplified but accurate spectral solar irradiance model. Theor. Appl. Climatol. 75, 203–212.

Paulescu, M., Schlett, Z., 2004. Performance assessment of global solar irradiation models under Romanian climate. Renew. Energy 29, 767–777.

Pawlak, D.T., Clothiaux, E.E., Modest, M.F., Cole, J.N.S., 2004. Full-spectrum correlated-k distribution for shortwave atmospheric radiative transfer. J. Atmos. Sci. 61, 2588–2601.

Perez, R., Ineichen, P., Moore, K., Kmiecik, M., Chain, C., George, R., Vignola, F., 2002. A new operational model for satellite-derived irradiances: description and validation. Solar Energy 73, 307–317.

Pinker, R.T., Frouin, R., Li, Z., 1995. A review of satellite methods to derive shortwave irradiance. Remote Sens. Environ. 51, 108–124.

Pinker, R.T., Kustas, W.P., Laszlo, I., Moran, M.S., Huete, A.R., 1994. Basin-scale solar irradiance estimates in semiarid regions using GOES 7. Water Resour. Res 30, 1375–1386.

Podestá, G.P., Nuñez, L., Villanueva, C.A., Skansi, M.A., 2004. Estimating daily solar radiation in the Argentine Pampas. Agric. Forest. Meteorol. 123, 41–53.

Pohlert, T., 2004. Use of empirical global radiation models for maize growth simulation. Agric. Forest. Meteorol. 126, 47–58.

Prescott, J.A., 1940. Evaporation from water surface in relation to solar radiation. Trans. Roy. Soc. Austr. 64, 114–125.

Revfeim, K.J.A., 1997. On the relationship between radiation and mean daily sunshine. Agric. Forest. Meteorol. 86, 181–191.

Sahin, A.D., Sen, Z., 1998. Statistical analysis of the Ångström formula coefficients and application for Turkey. Solar Energy 62, 29–38.

Suehrcke, H., 2000. On the relationship between duration of sunshine and solar radiation on the Earth's surface: Ångström's equation revisited. Solar Energy 68, 417–425.

Supit, I., van Kappel, R.R., 1998. A simple method to estimate global radiation. Solar Energy 63, 147–160.

Thornton, P.E., Running, S.W., 1999. An improved algorithm for estimating incident daily solar radiation from measurements of temperature, humidity, and precipitation. Agric. Forest. Meteorol. 93, 211–228.

Weiss, A., Hays, C.J., 2004. Simulation of daily solar irradiance. Agric. Forest. Meteorol. 123, 187–199.

Yang, K., Huang, G.-W., Tamai, N., 2001. A hybrid model for estimating global solar radiation. Solar Energy 70, 13–22.

Yang, K., Koike, T., 2002. Estimating surface solar radiation from upper-air humidity. Solar Energy 72, 177–186.